EVALUATING ERA5 WEATHER PARAMETERS DATA USING REMOTE SENSING AND IN SITU DATA OVER NORTH RED SEA

M. Ayman[1], Z. Salah[2], K. Tonbol[1], M. Shaltout[3] *

[1] AASTMT Arab Academy for Science and Technology and Maritime Transportation, Alexandria, Egypt
[2] General Scientific Research Department, EMA Egyptian Meteorological Authority, Cairo, Egypt
[3] Department of Oceanography, Faculty of Science, Alexandria University, Alexandria, Egypt

KEY WORDS: Red Sea, ERA5, Remote Sensing, Climate reanalysing, weather Characteristics, Numerical Weather Prediction.

ABSTRACT:

High demand is placed on atmospheric studies specially for climatic characteristics, in order to cooperate with the government vision for exploitation of marine resources and a great potential for renewable energy, including solar, wind, hydro and geothermal energy as well as the huge expansion in coastal construction projects planned in the Egyptian Red Sea coasts for establish and growth of industry, tourism and urbanization.
This study analyse the recent trends of Surface Wind (W10), surface air temperature (T2m), relative humidity (RH2m) and surface pressure (MSLP) using the European Centre for Medium-Range Weather Forecasts (ECMWF) latest fifth-generation reanalysis weather elements product global Reanalysis dataset (ERA5) Compared to Satellite Earth Observation (EO) altimetry remote sensing data (MERRA-2) and local observed data from chosen WMO automatic weather stations (AWS) over North Red Sea coasts in Egypt, Hourly data records were acquired from four WMO weather stations, deployed in different locations: Suez, Sharm Elshaikh, Safaga, Marsa Alam to study regional Climatic Characteristics, test and validate ERA5 data and evaluates the ability of ERA5 reanalysis to reproduce hourly and monthly averages for weather characteristics over North Red Sea, with hourly time series for data spans approximately 11 years, period from January 2012 to December 2022. Results of the analysis expected to reveal the agreement between remote sensing data, observations and ERA5 estimates, determine correlation values and Root Mean Square Error (RMSE).
Based on certain considerations outlined in this paper, it is appropriate to use MERRA-2 and ERA5 to characterize T2m, RH, W10 and MSLP over North Red Sea.

1. INTRODUCTION

1.1 Overview

Due to the lack of climatic studies and knowledge over the North East Red Sea area and the importance of the climatic characteristics for all human activities and due to the unique topography and hydrography of the Red Sea coasts over Egypt and due to the high impact of climate change all-over the globe its crucial to give more attention for climatic studies specially over such a promising areas.

Global studies for climate change mentioned that increase in temperature has impacts such as: increased incidence and severity of heat-waves, droughts. Over Egypt, there has been a number of mega heat waves in the last decade, particularly the record-breaking summers of 2010, 2012, 2015 and 2018, which caused the loss of life and severe economic damage to many sectors (e.g. agriculture, energy, water resources) (M. Eid, 2019)

1.2 Area of Study

Red Sea is a Longitudinal narrow semi-enclosed tropical body of water connected at the north with the Mediterranean through the Gulf of Suez and the Suez Channel and to the south with the Indian Ocean by strait of (Bab El Mandab), separating northeast Africa from Sinai Peninsula Lies between latitudes 30°N and 12° 30′N, Longitudes 33° and 44°E, with dimensions 1045 Nautical Mile long, 151 Nautical Mile average width (16-191 Nautical Mile), the total surface area of the Red Sea estimated between 438 and450 Km2, while the volume is between 215 and 251 Km3, The average depth is considered to be 491 m, The maximum depth recorded in the Red Sea is 2850 m which is small compared with oceans but it's large compared with such a body of water with its size (Gladstone, 2006) and is bordered by Egypt, Sudan, Eritrea and Djibouti on the west, and Yemen and Saudi Arabia on the east. Although the Red Sea is known for its natural beauty, with extensive corals reefs, South of Lat. 24° a deep incision, referred to as the axial trough, appears in the main basin.

This can be followed along the length of the Red Sea as far as 16°N. North of Lat. 22°N the coastal plains tend to be narrower (Nautical charts 158; 159, 2023) 500m contour is set back around 40 km from the coast, giving a wider coastal plain. From Egypt to the Sudanese border the coastline has large areas of sandy beaches, with far fewer areas of rocky coastline. Relatively straight coasts, few bays and inlets, no rivers discharge to continually taking materials into the Red Sea, have great effect on the continental dry climate in Africa. Wadis at various points along this coast carry runoff to the sea when occasional local rains fall. Most wadis are small. Further inland at a distance of 60 km from the coast occasional hills rise to 1,500 m or more (Gladstone, 2006). it is also an important shipping route for maritime transportation through the Suez Canal.

This study focused on Egyptian coasts over Northern Red Sea, coordinates latitudes (from 30° 30' N to 22° 00' N) and longitudes (from 32° 00' E to 39° 30' E) based on data from four (WMO) automatic weather stations (AWS) as shown in figure (1).

1.3 Data Collection

Data was collected from three main sources:
- European Centre for Medium-Range Weather Forecasts (ECMWF) latest fifth-generation reanalysis weather elements product global Reanalysis dataset (ERA5).
- Satellite Earth Observation (EO) altimetry remote sensing data (MERRA-2).
- Local observed data from chosen WMO automatic weather stations (AWS) over North Red Sea coasts in Egypt,

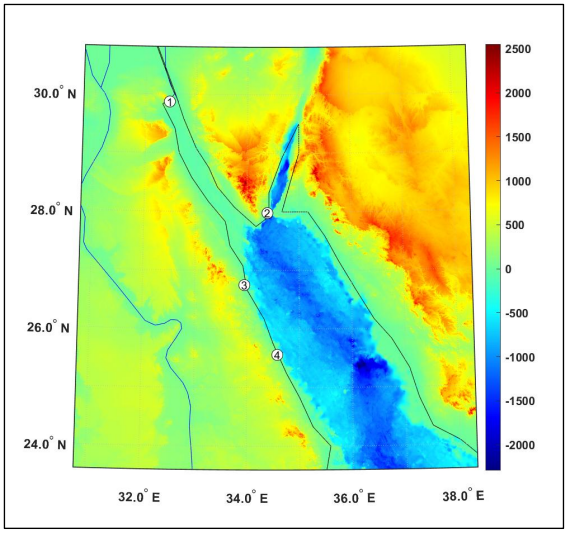

Figure 1. Bathymetric chart of the study area with the four considered weather observation stations: 1) Suez, 2)Sharm Elshaikh, 3) Safaga, 4) Marsa Alam. Regional winds are showed.

2. CLIMATIC BACKGROUND

2.1 Climatic Conditions

Semiarid climate According to the Koppen classification system, a system of climate classification using latitude band and degree of continentally as its primary forcing factors, a predominantly (BWh) type climate regime (the main climate is arid, the precipitation type is the desert type, and the temperature is high). This implies that the annual precipitation is less than 50% of this threshold, which factors in seasonal distribution of rainfall and the degree of dryness/coldness of the season and signified low-latitude climate (average annual temperature above 18°C) (Oliver, 2005).

Climatically, generally warm temperatures, dry summers, winter - dominated rainfall, and a profusion of microclimate due to local terrain, characterize the Red Sea.

2.2 Air temperature (T2m)

Average temperature increased in the eastern coast of Egypt because of the warm waves from the Arabian Peninsula and Eastern Mediterranean caused by warm Indian Monsoon low-pressure centre. In North Red Sea the air temperature exceeds the sea surface temperature by greatest value in the summer months, which is fairly influenced by conditions of an adjacent land. In winter air temperature is less than the sea surface by about half a degree. The mean diurnal range of air temperature is 4°C, from December to April, and 6°C in July, where 5°C in all other months, Generally maximum temperature occurs two hours after noon and minimum at sunrise, some changes happens because amount of heat lost by Earth at day or night (Hamed, 2002).

More incoming solar radiation (insolation) occurs with smaller incident angle when moving to the equator, the longer day time in summer months gives more radiation, over the area of study, maximum insolation happens in July and minimum in January. Rocks and sand land have very high albedo, which increase the daily temperature variation.

Due to rapid laps rate, altitude of the observed area is one of the most important factors in determining Air temperature, high slope of the mountains to the sea side has huge effect of the temperature over the mountains areas which is adjacent to the coast, while the narrow coastal plain makes the declination is neglected at the Red Sea coast.
Monthly averages for observed temperature over the area of study are shown in figure (2)

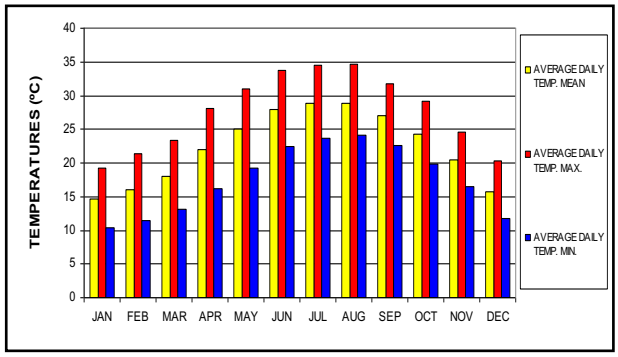

Figure 2. monthly averages temperature at North Red Sea in ºc
Source: Egyptian Naval Hydrographic Department, 2022

2.3 Wind Regime (W10)

Along the Red Sea coast, winds blow predominantly (65-70%) from the directions (N, NW and W). Winds from North Easterly directions occur during (10 – 15%) of time and the rest from the other direction. Speed average 5 –15 knots most of the year with higher velocities from North Westerly directions. Extreme winds occur in storms of which about 15 knots passes during a winter. The most effective wind direction to ships at port is South-Easterly wind because it brings swell, especially with high wind speeds.

The main body of the Red Sea, between latitude 16°N and 26°N, more than 75% of winds in all months of the year are of force 4 or less (0-16knots), and in the summer and autumn months this figure rises generally to over 80% and may exceed 85%. The mean annual wind speed is less than 10 knots and gales are rare. In most months the wind is observed as “calm” (less than 1 knots), on more than 5% of occasions, In the North Red Sea area, winds of force 5-6 (17-27knots) account for about 10% of observation in the summer and about 20% in mid-winter. The region of North Red Sea, including the Gulf of Suez, tends to have strongest wind throughout the year than the area just described. In the months, winds of force 4 or less occur between 60% and 70% of the time. The mean annual speed is a little over 10 knots and September is the windiest, and all winds appear to be rather higher on the Egyptian side. Winds of force 5-6 usually account for some 20-25% of observation. This figure is varying from about 15% in mid-winter to about 35% in September. Occasional gales occur throughout the year with isolated instance of force 11 to 12 being on record.

The prevailing wind directions over seasons are North to Northwest can be summarized as following:

a. During winter it’s clear that Northwest winds dominate over the Red Sea and rarely at night times Southwest.
b. During summer, the Northwest winds dominate the area with a percentage frequency of occurrence greater than that during winter.
c. During both spring and autumn, as transitional season, the Northwest winds also dominate over North Red Sea.

Monthly averages for (W10) over the North Red Sea are represented in wind roses in figures (3) and (4).

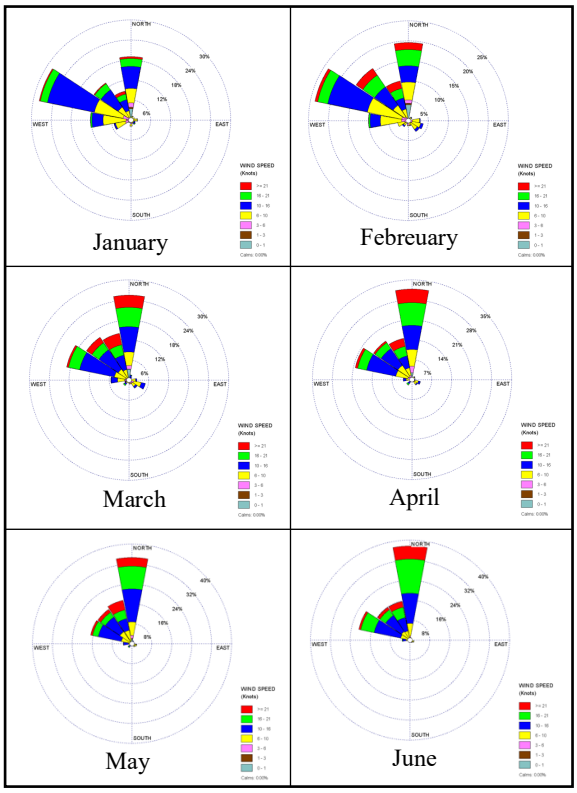

Figure 3. average wind direction and speed (January to June) Source: (Saad, 2010)

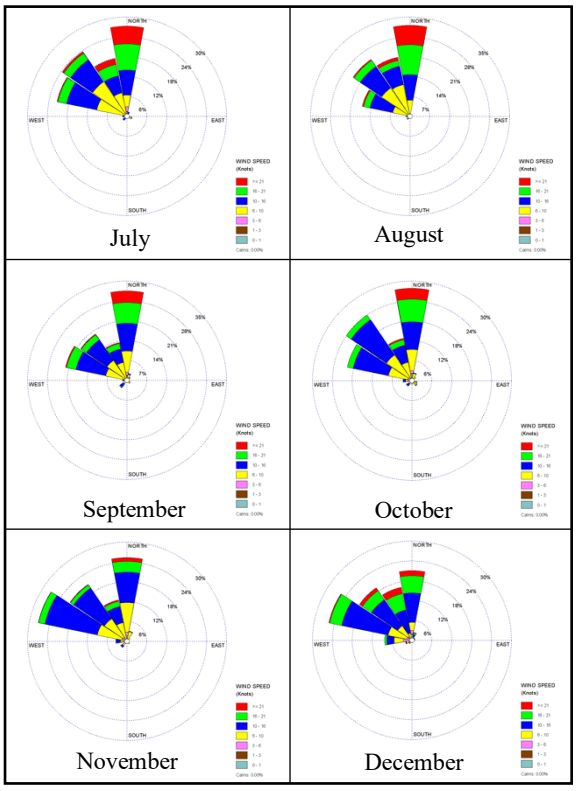

Figure 4. average wind direction and speed (July to December) Source: (Saad, 2010)

According to Kirchhoff's low and Wein's low, Continental terrain is good absorber and emitter to insolation, gain and lose temperature quickly which increases the diurnal laps rate, Positive laps rate during daytime increases the atmospheric instability and negative laps rate during night makes the atmosphere more stable (USAF 2022).

At the Red Sea coast wind tends to veers and increases speed in the period between sunrise and noon, backs and reduces speed through night. Diurnal average surface wind speeds in knots over North Red Sea shown in figure (5)

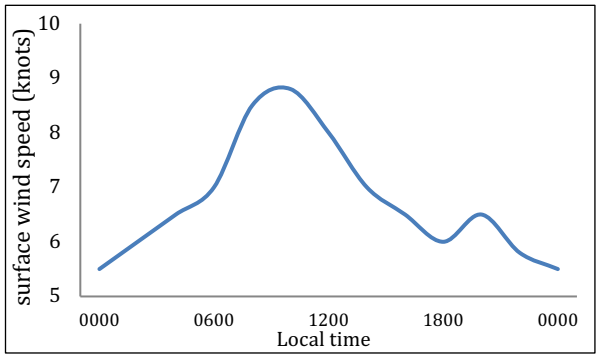

Figure 5. Diurnal average wind speed over North Red Sea Source: (Langodan, 2017)

2.4 Relative Humidity (RH)

Relatively low humidity for a coastal area as the prevailing wind almost parallel to the coastline and the dry continental nature for the land area, most dry in summer at the morning and most humid in winter at night.

Although most of the air that enters the Red Sea basin is fairly dry the area has reputation for hot, moist conditions, which render any prolong human activity very difficult. The apparent paradox is explained by the very height rate of evaporation from the warm waters of the Red Sea, Which raise the humidity of the lower layer of the atmosphere. Over the open sea the average annual relative humidity is about 70% with range annual 5% and a daily of maximum 4%. Average evaporation rates and relative humidity shown in table (1) and figure (6) respectively.

Station / Month	Suez	Safaga	Marsa Alam
January	3.9	5.2	5
February	4.2	5.7	5.5
March	5.6	6.3	6.1
April	6.8	7.3	6.5
May	7.3	8.5	7.3
June	8.2	9.8	8.3
July	7.8	9.3	7.3
August	6.7	9.1	7.4
September	6.6	8.4	7.2
October	16.2	6.6	6.1
November	4.7	5.6	5.6
December	4	5.1	5.1

Table 1. Average evaporation rate in millimetre measured by (Piche) instrument. Source: (Saad, 2010)

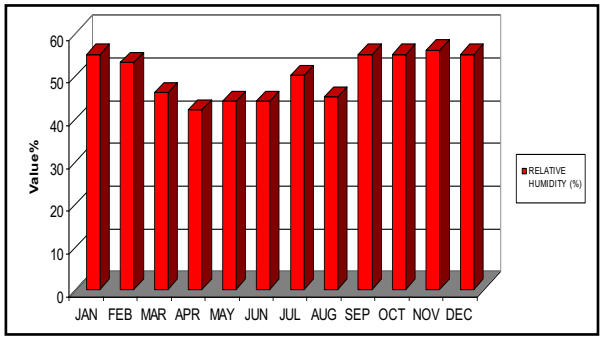

Figure 6. Monthly average relative humidity over North Red Sea Source: Egyptian Naval Hydrographic Department, 2023.

As shown in fig. (7) the diurnal humidity variation determined by absolute humidity and air temperature, in morning the rate of temperature increase more than the increase of the absolute humidity and vice versa during night time. Relative humidity inversely proportional with air temperature and the maximum happens at sunrise and the minimum value two hours after noon. The temperature, absolute humidity and the relative humidity diurnal varies with passing of more humid air mass during wind direction changes.

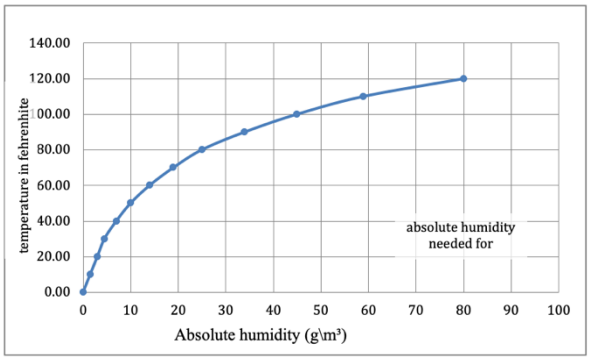

Figure 7. Relation between temperature and absolute humidity needed for air to be saturated, Source: USAF, 2022.

3. DATA USE AND METHODS OF ANALYSIS

3.1 Data

3.1.1 ERA5 weather parameters data: ERA5 is the fifth generation of the European Centre for Medium-Range Weather Forecasts (ECMWF) global climate reanalysis. The ECMWF's most recent reanalysis output is this dataset. The ERA5 reanalysis includes the modern observation period, ERA5 data on single levels from 1940 to present with daily updates. Hourly analysis fields in ERA5 data have a horizontal resolution of reanalysis 0.25° × 0.25° (atmosphere), allowing users to assess historical atmospheric and oceanic states.

Data of (U, V, RH2, T2m) were obtained from ERA5 for 11 years period from January 2012 to December 2022 on an hourly basis with a spatial resolution of 0.25° × 0.25°. These data were used to evaluate the ERA5 reanalysis to gain confidence and give a full image of these variables over the study area. This was done according to Copernicus Climate Change Service (C3S, 2023) and Hersbach et al. (2023).

ERA5 monthly averaged Eastward (U), Northward (V) component of wind at a height of 10m and hourly temperature of air at 2m above the surface (T2m) Over the study area for the given time series shown on Figures (8,9) respectively using historical climate statistics interface (ERA5 explorer) available online:(https://cds.climate.copernicus.eu/cdsapp#!/software/app-era5-explorer?tab=app). Relative humidity at a height of 2metres above the surface (the amount of water vapour present in air expressed as a percentage of the amount needed for saturation at the same temperature) shown on figure (10) using Agrometeorological indicator explorer and data extractor online: (https://cds.climate.copernicus.eu/cdsapp#!/software/app-agriculture-agera5-explorer-data-extractor?tab=app).

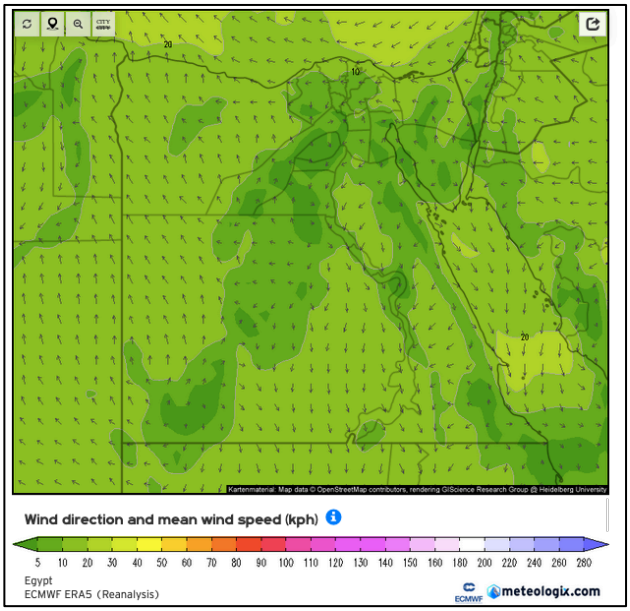

Figure 8. ERA5 l of (W10), time period (2011 – 2021) Source: (ECMWF, accessed on May 13, 2023)

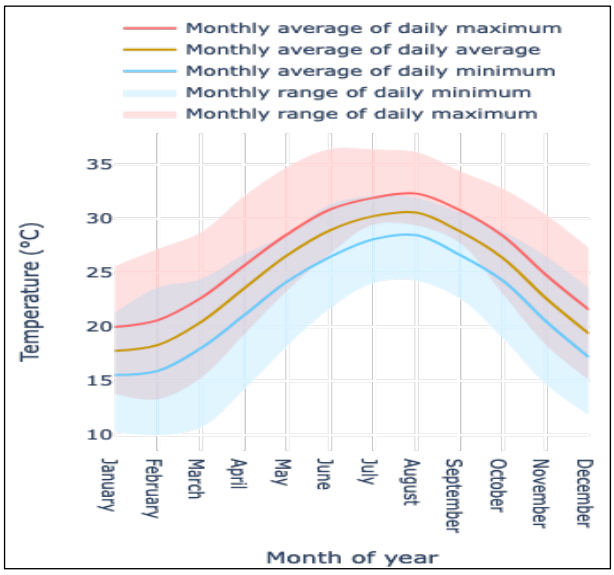

Figure 9. ERA5 Temperature average over North Red Sea (T2m) Source: (Hersbach et al., 2023)

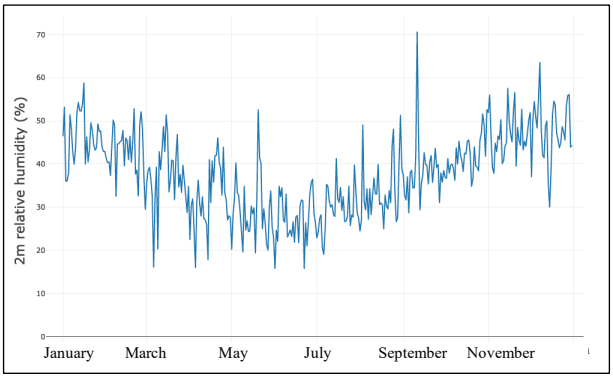

Figure 10. Era5 average Relative Humidity (RH2) Over North Red Sea, Source: (Hersbach et al., 2023) using (CSVplot).

3.1.2 Remote Sensing (Altimetric) Data: Remote sensing data were obtained from the National Aeronautics and Space Administration (NASA) Langley Research Centre for Prediction Of Worldwide Energy Resources (POWER) funded through the NASA Earth Science Directorate Applied Science Program which Provides solar & meteorological data.

The meteorological data/parameters in POWER Release 8 were based upon the Goddard's Global Modeling and Assimilation Office (GMAO) Modern Era Retrospective-Analysis for Research and Applications (MERRA-2) assimilation model products and GMAO Forward Processing – Instrument Teams (FP-IT) GEOS 5.12.4; MERRA-2 data based data/parameters were based upon satellite observations with subsequent inversion to surface solar insolation by NASA's Global Energy and Water Exchange Project (GEWEX). The horizontal resolution of the meteorological data sources are 0.5° x 0.625° latitude/longitude grid.

Remote Sensing data for Weather parameters (W10, RH2, T2m and MSLP) over the study area (Suez, Sharm Elshaikh, Safaga and Marsa Alam) averages for 11 years period (January 2012 to December 2022) shown in figures (11,12,13 and 14) respectively.

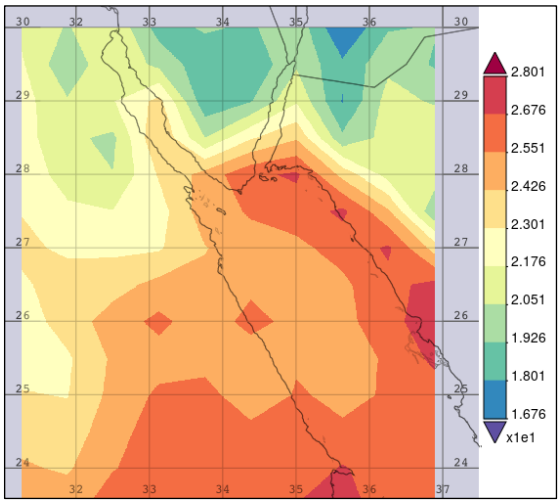

Figure 11. MERRA-2 (T2m) , time period (2011 – 2021)
Source: (www.giovanni.gsfc.nasa.gov, accessed on july 7, 2023)

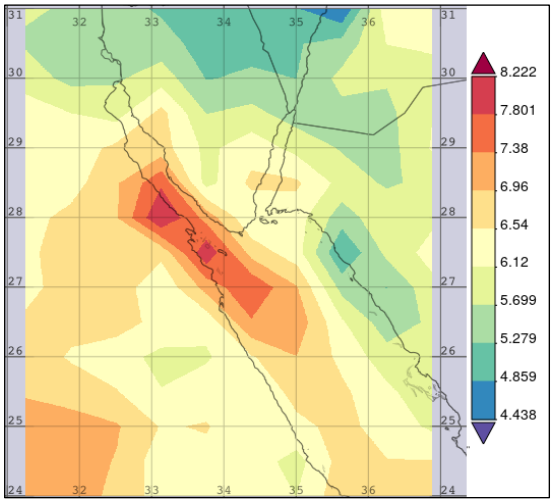

Figure 12. MERRA-2 (W10s) in m/sec, time period (2011-2021)
Source: (www.giovanni.gsfc.nasa.gov, accessed on july 7, 2023)

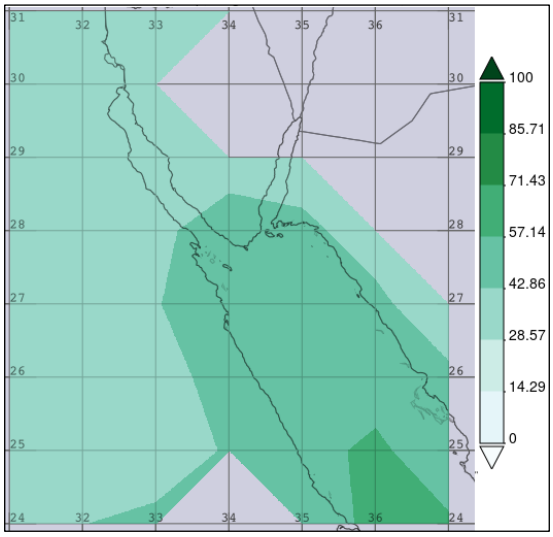

Figure 13. MERRA-2 (RH) in %, time period (2011 – 2021)
Source: (www.giovanni.gsfc.nasa.gov, accessed on july 7, 2023)

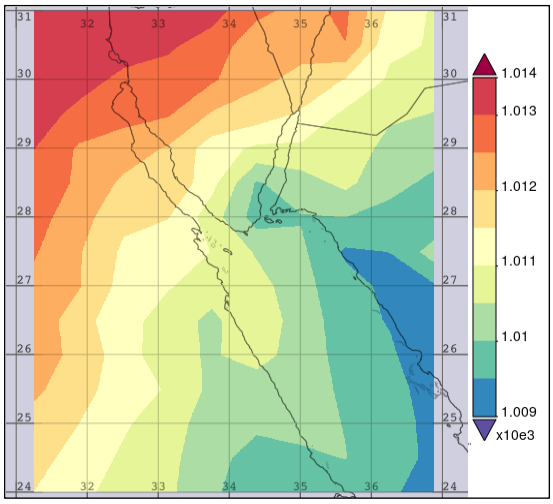

Figure 14. MERRA-2 (MSLP) in mbar, time period (2011–2021)
Source: (www.giovanni.gsfc.nasa.gov, accessed on july 7, 2023)

In situ (observed) Data: Weather parameters (W10, RH2, T2m) were collected from 4 chosen WMO automatic weather stations (AWS) distributed over the study area (Suez, Sharm Elshaikh, Safaga and Marsa Alam) were used to evaluate the ERA5 datasets. The location of the weather stations and the details of the stations are shown in Table (2). The average data for 11 years period (January 2012 to December 2022) are

shown in figures (15,16,17) respectively.

Station		International Station Number	Geographic Position		Number of observations	Height Above Sea Level (m)
Name	SN		Latitude	Longitude		
Suez	1	62450	29° 52` 14``	32° 28` 30``	95762	13.48
Sharm Elshaikh	2	62460	27° 58` 38``	34° 23` 42”	91645	50
Safaga	3	62466	26° 25` 08``	33° 57` 08``	96330	18
Marsa Alam	4	62470	25° 33` 26``	34° 35` 1``	71644	77

Table 2. Positions and elevations of meteorological stations
Source: Egyptian Meteorology Authority (EMA), 2023

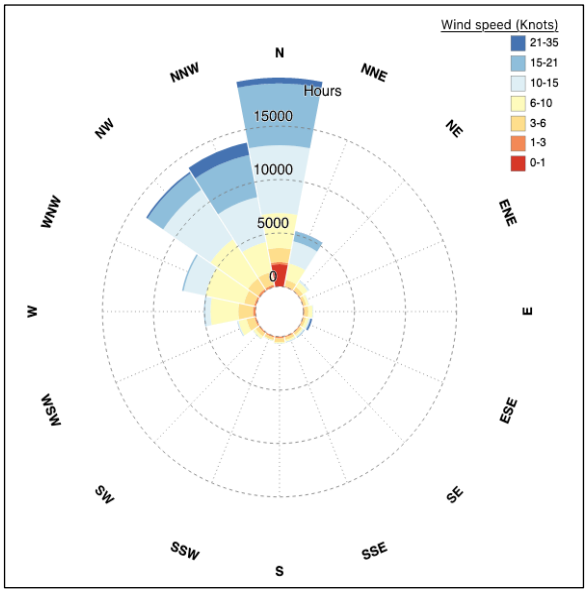

Figure 15. Wind average observations for the study area
Source: observed in-situ visualized using (windrose.xyz)

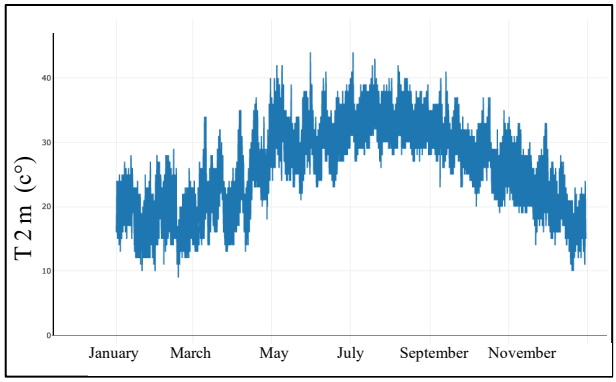

Figure 16. Temperature average over North Red Sea (T2m),
Source: observed in-situ visualized using (CSVplot)

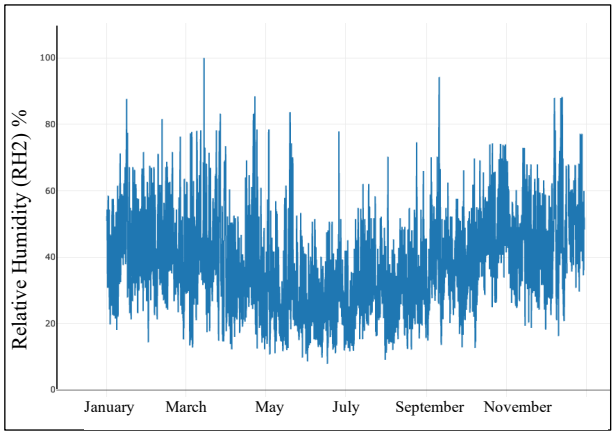

Figure 17. Relative humidity average over North Red Sea (RH2),
Source: observed in-situ visualized using (CSVplot)

3.2 Methods of analysis

To evaluate the quality of the ERA5 reanalysis data set for the North Red Sea area, ERA5, remote sensing and in situ data were collected. For data preparation the dataset was categorized and inspected for spikes, outliers, and incorrect data readings before smoothing.

As a quantitative research, descriptive statistical analysis method were used for data preparation, processing, analyzing and visualization using the following computer software: (Matlab, Excel, CSVploter, Windrose.xyz, ERA5 explorer and Agrometeorological indicator explorer and data extractor)

correlation coefficient (r) used as one of the metric criteria for the remote sensing, observed and reanalysis dataset, and root-mean-square-error (RMSE) were used to focus on errors, the relative bias (BIAS) are synthesis indices described by the correlation component and bias which were computed to investigate the relationship between the ERA5 reanalysis, remote sensing data and observed data at the 4 meteorological stations at hourly temporal scale.

4. RESULTS

4.1 Descriptive analysis for weather parameters

According to MERRA-2 remote sensing data, ERA5 reanalysis Data and in situ data, Table 3 shows the relation between MERRA-2, ERA5 and the observations at various positions. maximum & minimum ranges, difference in variation, standard deviation, mean values of the parameters [surface air temperature (T2m, c°), relative humidity (RH %), wind speed (WS_{10}, m/sec) and mean sea level pressure (MSLP, hpa)] were determined by descriptive statistics. After processing the collected meteorological data in excel, results have been identified for a particular stations that helps in proceeding with the comparison analysis.

Variables			n	R (%)	Minimum	Maximum	Annual mean ± standard deviation
Surface air temperature (T2m, c°)	Suez	In situ	95762	---	1.72	41.08	22.82 ± 6.06
		MERRA-2	96329	78	3.28	44.1	21.67 ± 7.83
		ERA5	95864	86.2	0.21	43.2	24.2 ± 7.31
	Sharm Elsheikh	In situ	91645	---	2	46	26.85 ± 6.58
		MERRA-2	96431	95.2	8.4	44	26.27 ± 6.76
		ERA5	96432	97.7	4.27	42.51	26.63 ± 6.44
	Safaga	In situ	96327	---	0.3	36.4	26.12 ± 12.3
		MERRA-2	96326	42.1	5.51	42.93	24.3 ± 7.22
		ERA5	96432	45.1	0.16	38.25	25.64 ± 5.52
	Marsa Alam	In situ	71644	---	5.32	45	25.86 ± 6.24
		MERRA-2	96431	95.78	10.48	41.4	26.08 ± 5.34
		ERA5	96432	97.4	6.4	41.52	25.83 ± 6.4
Variables			n	R (%)	Minimum	Maximum	Annual mean ± standard deviation
Relative Humidity (RH %)	Suez	In situ	96330	---	6.3	99.2	51.64 ± 16.2
		MERRA-2	96430	52	4.48	100	48.22 ± 5.2
		ERA5	96432	77	7.18	99.9	60.14 ± 15.95
	Sharm Elsheikh	In situ	91586	---	3.97	100	40.77 ± 15.44
		MERRA-2	96432	53.5	10.4	100	41.56 ± 13.86
		ERA5	96432	63.1	8.05	97.53	40.28 ± 12.29
	Safaga	In situ	96330	---	2.6	98.6	42.98 ± 13.37
		MERRA-2	96329	35.3	8.3	100	42.97 ± 16.83
		ERA5	96432	45	14.24	98.25	46.77 ± 10.93
	Marsa Alam	In situ	71598	---	3.2	100	41.23 ± 16.31
		MERRA-2	96431	71.59	12.8	100	52.37 ± 12.49
		ERA5	96432	77.3	3.9	99.84	42.84 ± 15.87
Variables			n	R (%)	Minimum	Maximum	Annual mean ± standard deviation
Surface Wind Speed (WS_{10}, m/s)	Suez	In situ	95593	---	0	11.32	3.77 ± 2.22
		MERRA-2	96431	47	0.02	14.8	3.94 ± 1.66
		ERA5	95864	55	0.02	11.62	3.25 ± 1.45
	Sharm Elsheikh	In situ	96432	---	0.0	6.91	4.38 ± 2.68
		MERRA-2	96432	83	0.02	14.98	4.44 ± 2.25
		ERA5	96432	52.5	0.0	5.82	2.12 ± 1.11
	Safaga	In situ	96428	---	0.01	13.4	5.2 ± 1.98
		MERRA-2	96431	51.38	0.01	15.5	5.21 ± 2.17
		ERA5	96432	68.5	0.04	12.9	5.12 ± 3.44
	Marsa Alam	In situ	71644	---	0.05	19.97	4.06 ± 1.78
		MERRA-2	96431	35.4	0.01	16.03	5.1 ± 2.22
		ERA5	96432	44.8	0.006	13.74	4.17 ± 3.38
Variables			n	R (%)	Minimum	Maximum	Annual mean ± standard deviation
Mean Sea Level Pressure (SLP, hpa)	Suez	In situ	95864	---	997.5	1032	1013.8 ± 5.16
		MERRA-2	96431	97.3	996.4	1031.6	1013.57 ± 5.2
		ERA5	95864	97.6	997.02	1031.56	1013.5 ± 5.18
	Sharm Elsheikh	In situ	91656	---	996	1029	1010.64 ± 5.2
		MERRA-2	96431	99.31	992.5	1023.3	1010.64 ±5.2
		ERA5	96432	99.3	997.53	1028.39	1010.78 ± 5.3
	Safaga	In situ	96330	---	998.2	1028.6	1012.26 ± 5.1
		MERRA-2	96431	96.3	969	1026.7	1010.31 ± 4.5
		ERA5	96432	82.2	998.8	1028.4	1011.38 ± 5.2
	Marsa Alam	In situ	71608	---	999	1031	1011.56 ± 4.9
		MERRA-2	96431	98.4	993.3	1012.9	1010.17 ± 4.8
		ERA5	96432	98.9	999.15	1027.49	1011.47 ± 5

Table 3. Comparison analysis between observed and ERA5 weather variables over Suez, Sharm elShaikh, Safaga and Marsa Alam: n = number of observations, R = correlation coefficient.

As seen in (Table 3), By comparing both results of the weather parameters over the study area, the highest (T2m) occurs over Sharm Elsheikh with avg. mean (26.74 c°) and the minimum annual mean (23.51) over Suez. The most humid station is Suez with avg. RH (55.89%) and the minimum humid mean (40.53%) over Sharm Elsheikh. (WS_{10}) measured in (m/sec) showing that the highest wind speed over Safaga mean (5.16 m/sec) and the minimum mean over Suez (3.51 m/sec). Avg. (MSLP) over Suez (1013.6 hpa) and over Sharm Elsheikh (1010.71 hpa).

4.2 Root Mean Square Error (RMSE)

RMSE values represent the absolute error between the ERA5, MERRA-2 and observed values as shown in (table 4).

the calculation formula is described as follows.

$$RMSE = \sqrt{\frac{\Sigma(0_i - E_i)^2}{n}}$$

Where 0_i are the observed values; E_i are ERA5 values;
$\sum$ represents 'sum'; and n is the number of observations.

location	variables	(RMSE) between ERA5 and Observations	(RMSE) between MERRA-2 and Observations
Suez	Surface air temperature (T2m, c°)	2.09	4.8
	Relative Humidity (RH %)	14.09	13.6
	Surface Wind Speed (WS_{10}, m/s)	1.69	2.07
	Mean Sea Level Pressure (SLP, hpa)	1.69	0.91
Sharm Elsheikh	Surface air temperature (T2m, c°)	20.7	6.4
	Relative Humidity (RH %)	32.7	17.2
	Surface Wind Speed (WS_{10}, m/s)	2.73	2.95
	Mean Sea Level Pressure (SLP, hpa)	0.63	1.36
Safaga	Surface air temperature (T2m, c°)	1.42	3.7
	Relative Humidity (RH %)	13.32	14.3
	Surface Wind Speed (WS_{10}, m/s)	2.16	2.7
	Mean Sea Level Pressure (SLP, hpa)	0.67	17.2
Marsa Alam	Surface air temperature (T2m, c°)	1.24	13
	Relative Humidity (RH %)	9.63	9.8
	Surface Wind Speed (WS_{10}, m/s)	2.97	3.34
	Mean Sea Level Pressure (SLP, hpa)	0.63	42.7

Table 4. (RMSE) of ERA5, MERRA-2 with observations for (T2m, RH, WS10, MSLP) over Suez, Sharm elShaikh, Safaga and Marsa Alam.

SUMMARY AND CONCLUSIONS

this study evaluated the performance of Remote Sensing Altimetric Data MERRA-2 and ERA5 reanalysis T2m, RH, W10s and MSP data at four locations over the North Red Sea Basin around Egypt's South-East coast (Suez, Sharm Elshaikh, Safaga and Marsa Alam) by comparing the obtained data with in-situ weather stations observations with temporal range all-over different seasons for time-span 11 years (2011 – 2021).

The validation of ERA5 reanalysis was done against the in-sito observed data (using the nearest neighbour algorithm to select the nearest grid to the observed station) during the period time (2011–2021). Validation processes indicated that ERA5 successfully simulated the surface air temperature and wind field over the study area. Generally, MERRA-2 gave a similar accuracy to ERA5 in describing the surface T2m, RH, wind field and MSLP over the study area from 2011 to 2021. Moreover, and by comparing ERA5/MERRA-2 with the observations during hourly extreme conditions using RMSE analyses, it could be concluded that MERRA-2 showed better accuracy than ERA5 in simulating W10 and T2m during extreme events. Thus, the use of MERRA-2 proved to be a better tool than ERA5 to understand the weather variabilities during the extreme weather conditions over the study area.

In detail, MERRA-2 overestimated observed T2m, RH and W10s on average by 2.4 C°, 2.13% and 0.32 m/sec while ERA5 overestimated observed T2m and RH on average by 0.8 C° and 3.35% respectively over the four studied stations together.

Also MERRA-2 underestimated observed MSLP on average by 0.9 hpa while ERA5 underestimated observed W10s and MSLP on average by 0.99 m/sec and 0.4 hpa respectively over the four studied stations together.

On the study of 11-year record over North East Red Sea, winter of 2011 and 2018 was the coldest and warmest winters, respectively. In the same context, summer of 2014 and summer of 2021 were the coldest and warmest summers.

REFERENCES

Gladstone, W., 2006. State of the marine environment, Report for the Red Sea and Gulf of Aden, PERSGA, Jeddah, KSA.

A. M. Saad, 2010. Wave and wind conditions in the Red Sea, A numerical study using a third generation wave model, Geophysical Institute, University of Bergen, Norway

M. M. Eid, Elsaied H. Gad, and H. Abdel Basset, 2019. Temperature Analysis Over Egypt, Al-Azhar Bulletin of Science Vol. 30, No. 2, (December) 2019, pp. 13-30.

Oliver, J., E., 2005. Encyclopaedia of world climatology, Springer, Dordrecht, Netherlands.

Admiralty nautical chart no. 158, 2015. Berenice to Masamirit, the United Kingdom Hydrographic office, Taunton, UK.

Admiralty nautical chart no. 159, 2015. Suez to Berenice, the United Kingdom Hydrographic office, Taunton, UK.

Hamed, 2002. Meteorology for seafarers, Alexandria, Egypt.

USAF, 2022. Department of the Air Force. AFMAN 15-111, Surface Weather Observations.

Langodan, 2017. The climatology of the Red Sea – part 1: the wind, International Journal of Climatology Int. J. Climatol. 37: 4509–4517, Published online 12 May 2017 in Wiley Online Library (wileyonlinelibrary.com) DOI: 10.1002/joc.5103

Hersbach, H.; Bell, B.; Berrisford, P.; Hirahara, S.; Horanyi, A.; Muñoz-Sabater, J.; Nicolas, J.; Peubey, C.; Radu, R.; Schepers, D.; et al. 2020. The ERA5 global reanalysis. Q. J. R. Meteorol. Soc. 146, 1999–2049, https://doi.org/10.1002/qj.3803.

Hersbach, 2023. historical climate statistics interface (ERA5 explorer) available online: (https://cds.climate.copernicus.eu/cdsapp#!/software/app-era5-explorer?tab=app), accessed on may 13, 2023.

Boogaard, H., Schubert, J., De Wit, A., Lazebnik, J., Hutjes, R., Van der Grijn, G., 2020. Agrometeorological indicators from 1979 to present derived from reanalysis. Copernicus Climate Change Service (C3S) Climate Data Store (CDS). DOI: 10.24381/cds.6c68c9bb(https://cds.climate.copernicus.eu/cdsapp#!/software/app-agriculture-agera5-explorer-dataextractor?tab=app), accessed on may 13, 2023.